Geodesic quantum walks

Giuseppe Di Molfetta
CNRS, LIS, Aix-Marseille Université, Université de Toulon, 13007 Marseille, France

Victor Deng
Ecole Normale Superieure, Departement d'Informatique, 75005 Paris, France

(Received 23 February 2022; accepted 25 May 2022; published 13 June 2022)

We propose a family of discrete space-time quantum walks capable of propagating on any arbitrary triangulations. Moreover, we also extend and generalize the duality principle introduced by Arrighi *et al.* [Sci. Rep. **9**, 10904 (2019)], linking continuous local deformations of a given triangulation and the inhomogeneity of the local unitaries that guide the quantum walker. We proved that in the formal continuous limit, in both space and time, this family of quantum walks converges to the (1+2)D massless Dirac equation on curved manifolds. We believe that this result has relevance in both modeling and simulating quantum transport on discrete curved structures, such as fullerene molecules or dynamical causal triangulation, and in addressing fast and efficient optimization problems in the context of the curved space optimization methods.

DOI: 10.1103/PhysRevA.105.062420

I. INTRODUCTION

Classical random walks are well known to approximate Brownian motion and the continuous diffusion equation [1]. In 1960 Roberts and Ursell [2] argued that this is still true if the jiggling motion of small dust particles occurs on a curved space-time instead (such as in the proximities of a strong gravitational field). Later, in 1984, Varopoulos [3] proved rigorously that, for a compact Riemannian manifold, if a triangulation is given, there always exists a canonical way to define a random walk on the vertices of the triangulation which converges to the Brownian motion. This suggested, more than 30 years ago, that classical random walks on triangulations provide simple procedures to "discretize" diffusion processes on curved space. The quantum analog of random walks has also been proven capable of simulating by means of local unitary operations another phenomenon ubiquitous in nature, transport [4–6]. Quantum walks describe situations where a quantum particle is taking steps on a lattice conditioned on its internal state, typically a (pseudo) spin one-half system. The particle dynamically explores a large Hilbert space associated with the position of the lattice and allows us to simulate a wide range of physical phenomena. With quantum walks, the transport is driven by an external discrete operation (coin and shift), which sets it apart from other lattice quantum simulation concepts where transport typically rests on tunneling between adjacent sites: all dynamics processes are discrete in space and time. More in general, they have been extended to graphs [7] and simplicial complexes [8,9]. In the same way that classical random walks provide a discretization procedure for the diffusion equation, quantum walks discretize the Dirac equation [10], i.e., the wave equation that describes the motion of spin one-half systems (i.e., fermions) in a relativistically invariant way. There are essentially two ways to discretize transport on curved surfaces through the implementation of quantum walks. The first, more oriented towards quantum simulation on specific physical platforms, is to encode the space-time metrics in local unitaries, thus making them nonhomogeneous. This procedure would correspond to sampling from the continuous manifold a finite data set of size corresponding to the number of grid points. Indeed, one of the authors has already proved that quantum walks can efficiently integrate the curved dynamics of a single particle in continuous space-time and converge to the general covariant Dirac equation [11,12]. These results were obtained on one- and two-dimensional rectangular grids [13] and later extended to any spatial dimensions [14]. The other way is to consider a discrete curved surface, e.g., a nonhomogeneous triangulation and define a homogeneous quantum walk on it. This procedure is more oriented towards modeling a transport phenomenon on discrete curved structures such as fullerene molecules, which consist entirely of carbon and take the form of a hollow sphere, ellipsoid, or tubular.

Related work. The aforementioned two approaches, long separated, have recently been reconciled by one of the authors, proving that there is, in some specific cases, a duality between the continuous local deformation of a triangulation and the inhomogeneity of the local unitaries that guide the quantum walker [15]. However, it was possible to prove this duality principle only in the case of diagonal deformation matrices, which in the case of the space-time tensor, would correspond to synchronous metrics. In this paper we propose to extend this result to any nondiagonal metric and to valorize the previously introduced duality principle in its maximum generality. Moreover, our work recalls the so-called geodesic random walk, first introduced by Jørgensen [16] and recently extended to Finsler manifolds [17]. In such classical walks, in

the absence of coin degree of freedom, the space-time metrics coefficients are embedded in the spatial increments.

Motivations. There are numerous motivations to introduce the geodesic quantum walk (GQW). First is the emergence of massless Dirac fermions on graphenelike materials [18], and within crystals in general. Quantum transport within such materials may be the physical phenomena that we wish to model by GQWs. Another topic is related to topological states, which are well known to be nontrivial on triangular grids [19]. Moreover GQWs should allow us to model all sorts of topologies as simplicial complexes, and the duality principle would provide a simple procedure for their quantum simulation. Finally, yet another motivation for exploring nonflat geometries is general relativity. Simulating curved transport on space-time triangulation is reminiscent of the question of matter propagation in triangulated space-time, as arising, e.g., in causal dynamical triangulation [20] or loop quantum gravity [21]. Finally, irregular lattices and/or random graphs may also be of interest: can they be re-interpreted in geometrical terms, i.e., in terms of an effective metric? Let us precise that a rigorous classical limit of these quantum schemes, including the quantum gravity theories, is still lacking and that techniques such as coarse-graining quantum maps [22], in the context of quantum automata, would play a central role in order to derive the macroscopic classical dynamical equations in the thermodynamic limit.

The paper is organized as follows: In Sec. II we introduce the basic quantum walk over equilateral triangles and we recall how to derive the formal continuous limit in space and time. Then Sec. III is dedicated to extending the definition of the QW in a way that the local operators could take into account any arbitrary triangulations; this results in covering transport over curved null geodesics and we thus prove that, taking the formal continuous limit, we recover a transport equation in curved space-time, namely the general covariant Dirac equation. In Sec. IV we provide a summary and some perspectives.

II. QUANTUM WALKING OVER TRIANGLES

Here we first reviewed the uniform QW as introduced by one of the authors in [4]. The walker is defined on the edges of a regular triangular grid, which sets it apart from other QWs defined on triangles and honeycomb structures, where the QW lives on vertices. The triangles are equilateral with sides $k = 0, 1, 2$ as shown in Fig. 1. Each triangle v, at time j, hosts two $\mathbb{C}^3$ vectors, denoted by $(\psi^{0,v}_{j,k})_{k=0,1,2}$ and $(\psi^{1,v}_{j,k})_{k=0,1,2}$. As each edge of the lattice is shared by two triangles, we label each triangle with 0 or 1 such that any two adjacent triangles have different labels, and we assign coin states 0 to triangles labeled 0 and coin states 1 to triangles labeled 1. The generic state of the walker at a given time j' therefore reads

$$\Psi_{j'} = \sum_{v_0,k} \psi^{0,v_0}_{j',k} \left|k_{v_0}, 0\right\rangle + \sum_{v_1,k} \psi^{1,v_1}_{j',k} \left|k_{v_1}, 1\right\rangle, \tag{1}$$

where v_0 spans the 0-labeled triangles, v_1 spans the 1-labeled triangles, and k_v refers to the kth edge of triangle v. The QW dynamics is recovered by the sequential application of two unitary local operators: the first operator $\hat{C}_k$, namely the quantum coin, is applied over each of the two-component

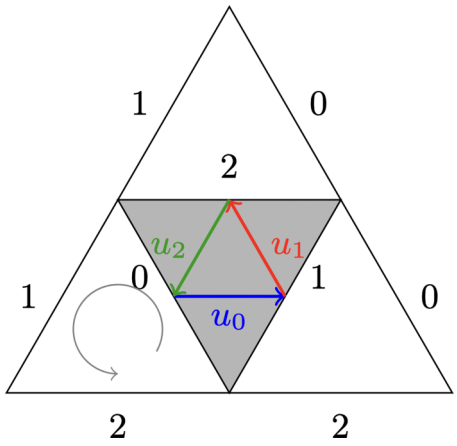

FIG. 1. The triangular QW: gray triangles are labeled 1, white ones are labeled 0.

wave functions lying on edges labeled k, for $k = 0, 1, 2$. The coin depends on k in general. The second operator R rotates every triangle anticlockwise, with component k of each triangle hopping to component $(k + 1) \bmod 3$, as shown in Fig. 1. Notice that it coincides with the simultaneous application of three shift operators S_{u_k}, along each unitary displacement vector u_k, $k = 0, 1, 2$, such that $R = \sum_{k=0}^{2} S_{u_k}$, as shown in Fig. 1. Each operator S_{u_k} acts on the edge k, internally to each triangle, moving the complex amplitude from the edge k to the edge $k + 1$. Let $\Psi^k = \sum_{v_0} \psi^{0,v_0}_k \left|k_{v_0}, 0\right\rangle + \sum_{v_1} \psi^{1,v_1}_k \left|k_{v_1}, 1\right\rangle$, we have, for each triangle v_0,

$$\begin{pmatrix} \left(S_{u_k} \Psi^k\right)^{0,v_0}_{k+1 \bmod 3} \\ \left(S_{u_k} \Psi^k\right)^{1,e(k,v_0)}_{k+1 \bmod 3} \end{pmatrix} = \begin{pmatrix} \psi^{0,v_0}_k \\ \psi^{1,v_0}_k \end{pmatrix}, \tag{2}$$

where $e(k, v)$ denotes the neighbor of triangle v along edge k. The overall shift operator can be written as follows:

$$S_{u_k} = \sum_{v_0} \left(\left|(k + 1 \bmod 3)_{v_0}, 0\right\rangle \left\langle k_{v_0}, 0\right| + \left|(k + 1 \bmod 3)_{e(k,v_0)}, 1\right\rangle \left\langle k_{v_0}, 1\right| \right). \tag{3}$$

Let us introduce the position $r := (x, y)$ as the center of each edge k_v, for a given triangle v. The two-component wave function $\Psi^v_{j,k}$ reads

$$\Psi_{j,k}(r) = \begin{pmatrix} \psi^0_{j,k}(r) \\ \psi^1_{j,k}(r) \end{pmatrix}, \tag{4}$$

and for a fixed k we therefore have

$$\begin{pmatrix} \left(S_{u_k} \Psi_k\right)^0_{k+1 \bmod 3}(r) \\ \left(S_{u_k} \Psi_k\right)^1_{k+1 \bmod 3}(r) \end{pmatrix} = \begin{pmatrix} \psi^0_k(r + \Delta u_k) \\ \psi^1_k(r - \Delta u_k) \end{pmatrix}, \tag{5}$$

where Δ is the lattice discretization step of the triangulation, i.e., half the length of an edge of the grid. It is also useful to relate the coordinate basis $\{u_k\}$, $k = 0, 1, 2$ to the rectangular coordinate system $\{u_s\}$, $s = x, y$:

$$u_k = \cos\left(\frac{2k\pi}{3}\right) u_x + \sin\left(\frac{2k\pi}{3}\right) u_y =: \mathcal{R}^s_k u_s, \tag{6}$$

where $\mathcal{R}$ is the coordinates change matrix.

Altogether, the triangular QW is given by the following recursive relations:

$$\Psi_{j+1,k} = \left(\prod_{i=0,1,2} S_{u_{k+i \bmod 3}} \hat{C}_{k+i \bmod 3}\right)\Psi_{j,k}. \tag{7}$$

We will now prove that by changing the coin basis and choosing a specific coin, we recover in the continuous space-time limit the massless Dirac equation in (2+1) dimensions.

Theorem II.1 (Dirac quantum walk over triangulation). Consider the previous quantum walk where

$$\hat{C}_0 = \hat{C}_1 = \hat{C}_2 =: \hat{C} = e^{i\pi/3}\mathcal{O}_z\left(-\frac{2\pi}{3}\right) = e^{i\pi/3}\exp\left(i\frac{\pi}{3}\sigma_z\right). \tag{8}$$

If $\tilde{\Psi}_k(t,r) = U\Psi_k(t,r)$, $C' = UCU^\dagger$ and $U = \exp(-i\alpha\sigma_y/2)C^2$ with $\alpha = -\arccos(\sqrt{5}/3)$, then the quantum walk in the new basis reads as

$$\tilde{\Psi}_{j+1,k} = \left(\prod_{i=0,1,2} S_{u_{k+i \bmod 3}} UCU^\dagger\right)\tilde{\Psi}_{j,k} \tag{9}$$

and, for $k = 0$, it admits as continuous limit in space-time, with discretization parameters $\Delta = \varepsilon$ for the spatial dimension and $\Delta_t = \varepsilon$ for the time dimension, the following partial differential equation:

$$\partial_t\Psi(t,x,y) = (\sigma_x\partial_x + \sigma_y\partial_y)\Psi(t,x,y). \tag{10}$$

Proof. By developing Eq. (5) around Δ, we obtain

$$(S_{u_k}\Psi)(r) = \Psi(r) + \Delta\sigma_z\partial_{u_k}\Psi(r) + o(\Delta). \tag{11}$$

Therefore, by developing Eq. (9) around ε, we get up to the first order:

$$\begin{aligned}&\tilde{\Psi}_0(t,r) + \varepsilon\partial_t\tilde{\Psi}_0(t,r)\\ &\quad= C'^3\tilde{\Psi}_0(t,r) + \varepsilon\big[C'^2\sigma_z C'\partial_{u_0}\tilde{\Psi}_k(t,r)\\ &\qquad + C'\sigma_z C'^2\partial_{u_1}\tilde{\Psi}_k(t,r) + \sigma_z C'^3\partial_{u_2}\tilde{\Psi}_0(t,r)\big] + o(\varepsilon).\end{aligned} \tag{12}$$

Then by reversing the basis change:

$$\begin{aligned}&\Psi_0(t,r) + \varepsilon\partial_t\Psi_0(t,r)\\ &\quad= U^\dagger C'^3 U\Psi_0(t,r)\\ &\qquad + \varepsilon(\tau_2\partial_{u_2} + \tau_1\partial_{u_1} + \tau_0\partial_{u_0})\Psi_0(t,r) + o(\varepsilon),\end{aligned} \tag{13}$$

where

$$\begin{aligned}\tau_0 &= C^2U^\dagger\sigma_z UC,\\ \tau_1 &= CU^\dagger\sigma_z UC^2,\\ \tau_2 &= U^\dagger\sigma_z U.\end{aligned} \tag{14}$$

We have $U^\dagger C'^3 U = U^\dagger(UCU^\dagger)^3U = C^3 = I_2$ with our choice of C. To prove the theorem, we therefore need

$$\sum_{i=0}^{2}\tau_i\partial_{u_i} = \sigma_x\partial_x + \sigma_y\partial_y. \tag{15}$$

We first translate the $(\partial_{u_i})_{i=0,1,2}$ in terms of the coordinates (x,y), using Eq. (6):

$$\partial_{u_k} = \cos\left(\frac{2i\pi}{3}\right)\partial_x + \sin\left(\frac{2i\pi}{3}\right)\partial_y = \mathcal{R}^s_k\partial_s. \tag{16}$$

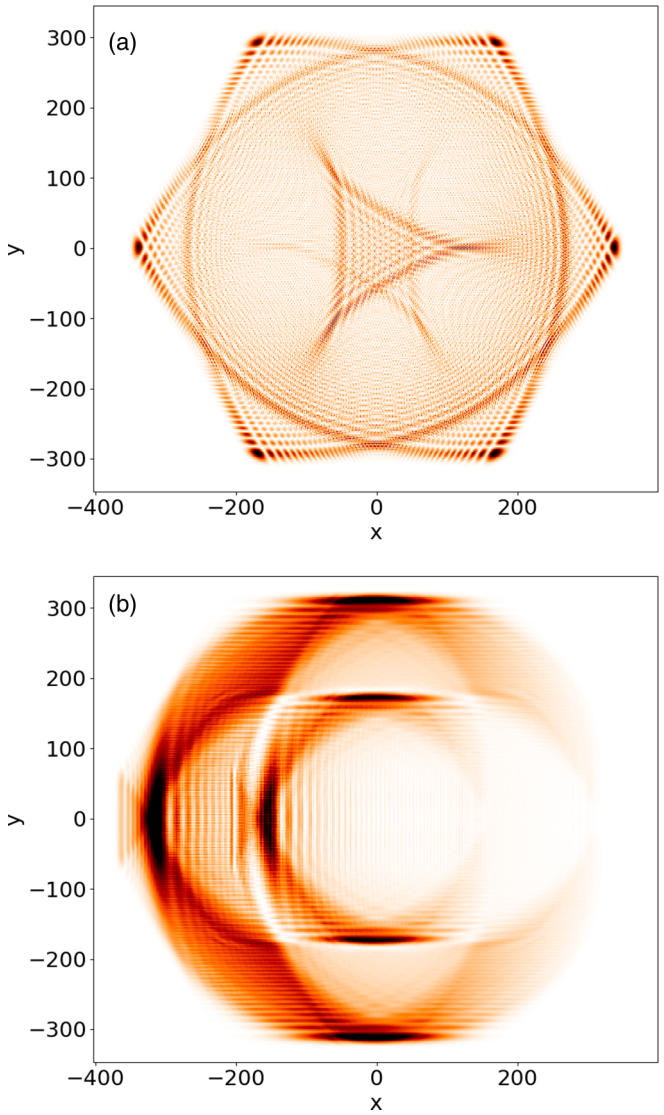

FIG. 2. (a) Simulation with initial amplitudes 1 on edge 0 of triangle (0,0) at 300 steps. (b) Simulation with an initially uniformly spread amplitude over a centered rectangle (size of the rectangle: a fifth of each dimension), sides 0 only, at 250 steps

We can then derive a relation between the τ_i and the σ^s:

$$\mathcal{R}^s_i\tau^i = \sigma^s, \quad s = x, y. \tag{17}$$

This equation, along with the unitarity and traceless condition on the τ_i, leads to the following unique τ_i matrices, up to a sign:

$$\begin{aligned}\tau_0 &= \frac{2}{3}\sigma_x + \kappa\sigma_z,\\ \tau_1 &= -\frac{1}{3}\sigma_x + \frac{\sqrt{3}}{3}\sigma_y + \kappa\sigma_z,\\ \tau_2 &= -\frac{1}{3}\sigma_x - \frac{\sqrt{3}}{3}\sigma_y + \kappa\sigma_z,\end{aligned} \tag{18}$$

with $\kappa = \pm\frac{\sqrt{5}}{3}$. By choosing $\kappa = \frac{\sqrt{5}}{3}$, and by using Eqs. (14) and (18):

$$\tau_0 = C^2U^\dagger\sigma_z UC = \tfrac{2}{3}\sigma_x + \kappa\sigma_z, \tag{19}$$

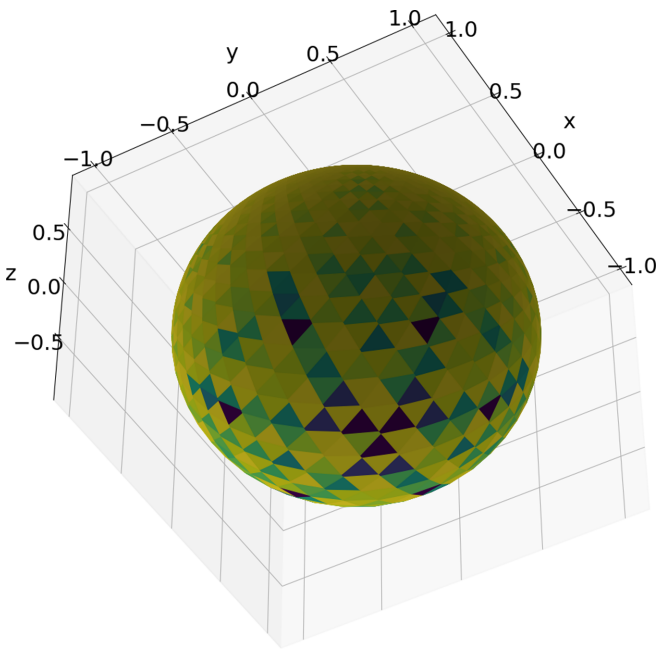

FIG. 3. Dirac quantum walker over the stereographically projected sphere after 80 steps.

we can derive $UC = \exp(-i\alpha\sigma_y/2)$ with $\alpha = -\arccos(\sqrt{5}/3)$, hence

$$U = \exp(-i\alpha\sigma_y/2)C^\dagger = \exp(-i\alpha\sigma_y/2)C^2,$$

where in the last sentence we used that C is unitary and $C^3 = I_2$ from the zeroth-order condition. Finally, notice that with the aforementioned choice of U and C, Eqs. (14), (18), and (19), are satisfied. Therefore, by taking the formal limit $\varepsilon \to 0$ in Eq. (13) and using Eq. (15), we recover the following Dirac equation in (2+1) dimensions:

$$\partial_t \Psi(t,x,y) = (\sigma_x\partial_x + \sigma_y\partial_y)\Psi(t,x,y). \tag{20}$$

■

We simulated the Dirac QW with different initial states. In each density plot, the color at a given point corresponds to the sum of the probability densities at each edge of the triangle at this point. All simulations were performed on grids of 802×400 triangles, with periodic conditions. The spatial coordinates shown on the axes are multiples of ε. In Fig. 2(a), whose initial state is concentrated in a single point, the walker propagates isotropically at unit speed. In Fig. 2(b), where the initial state is more spread, we can see a left-moving behavior along with vertical spreading (still at unit speed).

III. THE GEODESIC QUANTUM WALK

Simulating and modeling transport on physical molecules such as fullerenes requires taking into account the nonflat geometry of such structures. Let us consider, as an example, the triangulation of the sphere. A Dirac QW can be implemented on it, as shown in Fig. 3. Indeed, to recover the metrics of a unit sphere, we (conformally) project it onto a plane at $z = -1$, and we determine local orthonormal bases of the sphere that project onto orthogonal bases of the plane aligned with the axes. The inverse of the stereographical projection reads

$$\varphi(x,y) = \left(\frac{2x}{\frac{1}{2}(x^2+y^2)+2}, \frac{2y}{\frac{1}{2}(x^2+y^2)+2}, 1 - \frac{4}{\frac{1}{2}(x^2+y^2)+2}\right), \tag{21}$$

and its partial derivatives read

$$\frac{\partial\varphi}{\partial x} = \left(\frac{4(-x^2+y^2+4)}{(x^2+y^2+4)^2}, -\frac{8xy}{(x^2+y^2+4)^2}, \frac{16x}{(x^2+y^2+4)^2}\right),$$
$$\frac{\partial\varphi}{\partial y} = \left(-\frac{8xy}{(x^2+y^2+4)^2}, \frac{4(x^2-y^2+4)}{(x^2+y^2+4)^2}, \frac{16y}{(x^2+y^2+4)^2}\right). \tag{22}$$

Flattening a part of the sphere on a plane corresponds to deforming the local basis of the triangulation by

$$\Lambda(x,y) = \begin{pmatrix} 1/\left\|\frac{\partial\varphi}{\partial x}\right\|_2 & 0 \\ 0 & 1/\left\|\frac{\partial\varphi}{\partial y}\right\|_2 \end{pmatrix}. \tag{23}$$

Once the metrics is flattened, but deformed, we can implement the very same QW, introduced previously. We also know that, if the metrics is diagonal, as in the aforementioned example, and we are sufficiently far from the singularities [23], the curved transport of the walker can be simulated over a regular (i.e., nondeformed) triangulation, at the price of considering nonuniform evolution operators. In the following we will prove that there exists a more general family of QW that we call geodesic QW (GQW), capable of simulating *any* arbitrary deformed triangulation. Moreover, we introduce anisotropic space-time discretization in order to recover the most general curved Dirac equation in the continuous limit.

To begin with, let us explore the case of a global homogeneous deformation of the lattice. Such a transformation consists of a uniform change of basis of the following form:

$$u_i' = \begin{pmatrix} \lambda_{00} & \lambda_{01} \\ \lambda_{10} & \lambda_{11} \end{pmatrix} u_i =: \Lambda u_i, \tag{24}$$

meaning that $u_x' = \lambda_{00}u_x + \lambda_{10}u_y$ and $u_y' = \lambda_{01}u_x + \lambda_{11}u_y$.

The derivatives ∂_{u_i} also transform as

$$\partial_{u_i'} = \Lambda\partial_{u_i}. \tag{25}$$

By actually deforming the triangulation and using the Dirac QW defined in the previous section, that is by solving together (25) and (10), we get

$$\partial_t\psi = \{B^s, \partial_s\}\psi \tag{26}$$

with

$$B^x = \lambda_{00}\sigma^x + \lambda_{01}\sigma^y,$$
$$B^y = \lambda_{10}\sigma^x + \lambda_{11}\sigma^y, \tag{27}$$

or, with Eq. (6),

$$B^s = \Lambda^s_i\sigma^i = \Lambda^s_i R^j_i \tau_j, \tag{28}$$

where $\Lambda_i^s = \lambda_{si}$, 0 corresponds to x, and 1 corresponds to y. Then from Eq. (13) we get

$$\partial_t \Psi_k(t,r) = (\tau_2' \partial_{u_2} + \tau_1' \partial_{u_1} + \tau_0' \partial_{u_0}) \tag{29}$$

with

$$\begin{aligned}
\tau_0' &= \frac{2}{3}(\lambda_{00}\sigma_x + \lambda_{01}\sigma_y) + \kappa\sigma_z, \\
\tau_1' &= -\frac{1}{3}(\lambda_{00}\sigma_x + \lambda_{01}\sigma_y) + \frac{\sqrt{3}}{3}(\lambda_{10}\sigma_x + \lambda_{11}\sigma_y) + \kappa\sigma_z, \\
\tau_2' &= -\frac{1}{3}(\lambda_{00}\sigma_x + \lambda_{01}\sigma_y) - \frac{\sqrt{3}}{3}(\lambda_{10}\sigma_x + \lambda_{11}\sigma_y) + \kappa\sigma_z,
\end{aligned} \tag{30}$$

that is, we obtain the matrices τ_i' by applying the deformation Λ to the σ_x and σ_y coordinates of the matrices τ_i.

The velocity field remains uniform here. Now, in order to simulate an inhomogeneous velocity field, we need to choose a space-time-dependent $\Lambda(t,x,y)$ transformation. Instead of introducing this distortion on the lattice via the modification of the u_i vectors, the unitary matrices τ_i can be transformed into matrices $\beta_i(t,x,y)$ to produce the same effect. We indeed seek for a set of matrices $\beta^i(t,x,y)$ that fulfill the following conditions:

(C1) We impose that

$$\Lambda_k^j(t,x,y) R_i^k \tau^i = R_i^j \beta^i(t,x,y), \quad j = x,y. \tag{31}$$

We obtain this condition by equating expressions (28) and (17) (with τ^i replaced by β^i in the latter).

(C2) Each of the β^i has $\{-1,1\}$ as eigenvalues, i.e., at any time step and any point (x,y) of the lattice, there exist three unitaries $U_i(t,x,y)$ such that

$$\beta^i(t,x,y) = U_i^\dagger(t,x,y)\sigma_z U_i(t,x,y). \tag{32}$$

Note that condition (C1), which we call the duality condition, implies that the coordinate transformation dictated by $\Lambda_k^j(t,x,y)$ is transferred to the unitary operations $\beta^i(t,x,y)$, instead of the original τ^i. Additionally, condition (C2) will allow us to rewrite the QW evolution in terms of the usual state-dependent translation operators.

To lighten the notations, we will omit the space-time dependence both in these matrices and in the $U_i(t,x,y)$. The above conditions allow us to calculate the β^i matrices, which can be written as a combination of Pauli matrices, i.e., $\beta^i = \vec{n}^i \cdot \vec{\sigma}$, where each $\vec{n}^i$ must be a real, unit vector $\vec{n}^i = (\sin\theta_i, 0, \cos\theta_i)$ for some space-time-dependent angles θ_i. Moreover, we will see that the σ_y component is not needed to achieve our purpose.

In this way,

$$\beta_i = U_i^\dagger \sigma_z U_i = \begin{pmatrix} \cos\theta_i & \sin\theta_i \\ \sin\theta_i & -\cos\theta_i \end{pmatrix} \tag{33}$$

and by diagonalizing each β_i, we obtain

$$U_i(\theta_i) = \begin{pmatrix} \cos\frac{\theta_i}{2} & \sin\frac{\theta_i}{2} \\ -\sin\frac{\theta_i}{2} & \cos\frac{\theta_i}{2} \end{pmatrix}. \tag{34}$$

The most naive way to implement such a walk is by alternating the unitaries U_i and the shift operators as seen in the first section, where the unitaries were homogeneous due to an appropriate choice of the coin state basis and parameters. However, the unitaries will be three different ones, depending on three independent real parameters θ_i, which is not sufficient to simulate all possible deformations. In fact, each space-time-dependent Λ depends on four real free parameters. Thus, in order to recover this local deformation, we need at least one more internal parameter in the QW evolution. Moreover, terms like $\partial_j \lambda_{ij}$ are necessary to conserve the probability distribution of the walker. This can be achieved by iterating twice each unitary operator. All these considerations lead us to define the geodesic quantum walk operator as follows:

$$\Psi_{j+2,k} = Z_2 Z_1 \Psi_{j,k}, \tag{35}$$

where

$$\begin{aligned}
Z_1 &= H\left(\prod_{i=0,1,2} \bar{V}_{k+i \bmod 3}\right)\left(\prod_{i=0,1,2} V_{k+i \bmod 3}\right)H, \\
Z_2 &= Q^\dagger\left(\prod_{i=0,1,2} \bar{K}_{k+i \bmod 3}\right)\left(\prod_{i=0,1,2} K_{k+i \bmod 3}\right)Q,
\end{aligned} \tag{36}$$

and

$$\begin{aligned}
V_i &= U_i(\theta_i) S_{u_i} U_i(\theta_i)^\dagger, \\
\bar{V}_i &= U_i(\theta_i)^\dagger S_{u_i} U_i(\theta_i), \\
K_i &= U_{i+3}(\theta_{i+3}) S_{u_i} U_{i+3}(\theta_{i+3})^\dagger, \\
\bar{K}_i &= U_{i+3}(\theta_{i+3})^\dagger S_{u_i} U_{i+3}(\theta_{i+3}),
\end{aligned} \tag{37}$$

where

$$H = \frac{1}{\sqrt{2}}\begin{pmatrix} 1 & 1 \\ 1 & -1 \end{pmatrix}, \quad Q = \frac{1}{\sqrt{2}}\begin{pmatrix} 1 & -i \\ 1 & i \end{pmatrix}. \tag{38}$$

In practice, for edges labeled k, one step of the walk consists of first applying H to each edge, then applying $U_k[\theta_k(t,x,y)]^\dagger$ on each edge, then shifting along u_k, then applying $U_k[\theta_k(t,x,y)]$ on each $(k+1)$-*labeled* edge, then applying $U_{k+1}[\theta_{k+1}(t,x,y)]^\dagger$ on each $(k+1)$-labeled edge, and so on.

Let us discuss this choice. Each Z_i iterates two modified versions of the quantum walk seen in Sec. II, choosing different unitaries for each edge k of the triangle in order to get in the continuous limit spatial derivatives of the unitaries U_i. Notice that for the second iteration we have chosen the transpose conjugate of the unitaries U_i. This is justified by the fact that, in the end, we wish to recover spatial derivatives of the form $\partial_j \beta_i = (\partial_j U_i^\dagger)\sigma_z U_i + U_i^\dagger \sigma_z \partial_j U_i$. Iterating twice the same operator V_i or K_i would not be sufficient to recover the total derivative, and we would have twice $U_i^\dagger \sigma_z \partial_j U_i$. Finally, H and Q provide the change of basis in the coin state basis to recover in the continuous limit a true 2D propagation, similarly to the change of basis U in Sec. II. In conclusion, two of the Z_i are necessary to have enough free parameters for the deformation Λ.

Let us now prove that the GQW correctly converges to the Dirac equation in a $(2+1)$-curved space-time. To this scope we introduce the following anisotropic scaling following [24]:

$$\theta_i(t,x,y) = \frac{\pi}{2} + \varepsilon^{1/2} l_i(t,x,y), \quad \Delta_x = \varepsilon^{1/2}, \quad \Delta_t = \varepsilon \tag{39}$$

for some space-time-dependent functions l_i. By expanding Eq. (35) up to first order in ε, after a tedious but

straightforward computation, which we spare the reader from detailing here, one arrives to the following equation in the continuum limit $\varepsilon \to 0$:

$$\partial_t \Psi = \big[\partial_{u_2}(l_2\sigma_x + l_5\sigma_y) + \partial_{u_1}(l_1\sigma_x + l_4\sigma_y) + \partial_{u_0}(l_0\sigma_x + l_3\sigma_y)\big]\Psi + \big[(l_2\sigma_x + l_5\sigma_y)\partial_{u_2} + (l_1\sigma_x + l_4\sigma_y)\partial_{u_1} + (l_0\sigma_x + l_3\sigma_y)\partial_{u_0}\big]\Psi. \quad (40)$$

Now, using Eq. (25), we can reformulate the above equation in terms of ∂_x and ∂_y and link the coefficients $l_i(r)$ and $\lambda_{ij}(r)$:

$$\partial_t \Psi = \partial_x(\lambda_{00}\sigma_x + \lambda_{01}\sigma_y)\Psi + (\lambda_{00}\sigma_x + \lambda_{01}\sigma_y)\partial_x\Psi + \partial_y(\lambda_{10}\sigma_x + \lambda_{11}\sigma_y)\Psi + (\lambda_{10}\sigma_x + \lambda_{11}\sigma_y)\partial_y\Psi, \quad (41)$$

where

$$\lambda_{00} = -\frac{1}{2}(l_2 + l_1) + l_0,$$
$$\lambda_{01} = -\frac{1}{2}(l_5 + l_4) + l_3,$$
$$\lambda_{10} = -\frac{\sqrt{3}}{2}(l_2 - l_1),$$
$$\lambda_{11} = -\frac{\sqrt{3}}{2}(l_5 - l_4), \quad (42)$$

which coincides with the curved Dirac equation, in its canonical form [25]. Notice that we simply recover Eq. (26) for homogeneous Λ. Moreover, observe that we have a system of linear equations which is overdetermined, which leaves us enough freedom to recover the deformation matrix we wish. For instance, a good choice to gauge away this ambiguity is $l_5 = -l_4$ and $l_2 = -l_1$, which leads to the unique choice:

$$l_0 = \lambda_{00}, \quad l_1 = \frac{\lambda_{10}}{\sqrt{3}}, \quad l_3 = \lambda_{01}, \quad l_4 = \frac{\lambda_{11}}{\sqrt{3}}. \quad (43)$$

We have thus proven that a nonhomogeneous arbitrary deformation of the triangulation can be simulated by local nonhomogeneous unitaries applied on the edges of a homogeneous regular triangulation.

IV. CONCLUSION

A more general family of QWs on triangulations has been introduced. We have shown that it is possible to relate quantum transport on curved surfaces to a quantum simulator, on regular triangular grids, based on a nonuniform spatial distribution of local unitaries. GQWs are a nontrivial generalization of the well-known geodesic random walkers, where the metric is embedded in the displacement operators. We believe that this result has relevance for both modeling and simulating quantum transport on discrete structures, such as fullerene molecules. Moreover, we aim, in the next future, to address fast and efficient optimization problems by using quantum curved space optimization methods, inspired by the aforementioned results. Indeed, we know that spatial search and optimization algorithms are often reformulated in terms of quantum walk. Recently curved space optimization algorithms based on classical random walks on curved surfaces have been introduced) [26,27]. We believe that our model could therefore be used to gain a polynomial advantage over classical computation times. Although pertinent, this development will be the subject of a forthcoming research paper.

The source for C++ code for all the simulations included in this paper is freely accessible at [29].

[1] F. B. Knight, On the random walk and Brownian motion, Trans. Amer. Math. Soc. **103**, 218 (1962).

[2] P. H. Roberts and H. D. Ursell, Random walk on a sphere and on a Riemannian manifold, Philos. Trans. R. Soc. London A **252**, 317 (1960).

[3] N. T. Varopoulos, Brownian motion and random walks on manifolds, Ann. l'institut Fourier **34**, 243 (1984).

[4] P. Arrighi, G. Di Molfetta, I. Márquez-Martín, and A. Pérez, Dirac equation as a quantum walk over the honeycomb and triangular lattices, Phys. Rev. A **97**, 062111 (2018).

[5] J. Mareš, J. Novotný, and I. Jex, Quantum walk transport on carbon nanotube structures, Phys. Lett. A **384**, 126302 (2020).

[6] G. Jay, F. Debbasch, and J. Wang, A systematic method to building Dirac quantum walks coupled to electromagnetic fields, Quant. Info. Proc. **19**, 422 (2020).

[7] A. D. Verga, Interacting quantum walk on a graph, Phys. Rev. E **99**, 012127 (2019).

[8] K. Matsue, O. Ogurisu, and E. Segawa, Quantum walks on simplicial complexes, Quant. Info. Proc. **15**, 1865 (2016).

[9] Q. Aristote, N. Eon, and G. Di Molfetta, Dynamical triangulation induced by quantum walk, Symmetry **12**, 128 (2020).

[10] P. Arrighi, V. Nesme, and M. Forets, The Dirac equation as a quantum walk: Higher dimensions, observational convergence, J. Phys. A: Math. Theor. **47**, 465302 (2014).

[11] P. Arrighi, G. Di Molfetta, and S. Facchini, Quantum walking in curved spacetime: Discrete metric, Quantum **2**, 84 (2018).

[12] G. Di Molfetta, M. Brachet, and F. Debbasch, Quantum walks as massless Dirac fermions in curved space-time, Phys. Rev. A **88**, 042301 (2013).

[13] P. Arnault and F. Debbasch, Quantum walks and gravitational waves, Ann. Phys. **383**, 645 (2017).

[14] P. Arrighi and F. Facchini, Quantum walking in curved spacetime: (3+1) dimensions, and beyond, Quantum Inf. Comput. **17**, 0810 (2017).

[15] P. Arrighi, G. Di Molfetta, I. Marquez-Martin, and A. Perez, From curved spacetime to spacetime-dependent local unitaries over the honeycomb and triangular quantum walks, Sci. Rep. **9**, 10904 (2019).

[16] E. Jørgensen, The central limit problem for geodesic random walks, Z. Wahrscheinlichkeitstheorie Verw. Geb. **32**, 1 (1975).

[17] T. Ma, V. S. Matveev, and I. Pavlyukevich, Geodesic random walks, diffusion processes and Brownian motion on Finsler manifolds, J. Geometric Anal. **31**, 12446 (2021).

[18] K. S. Novoselov, A. K. Geim, S. V. Morozov, D. Jiang, M. I. Katsnelson, I. Grigorieva, S. Dubonos, and A. Firsov, Two-dimensional gas of massless Dirac fermions in graphene, Nature (London) **438**, 197 (2005).

[19] T. Kitagawa, M. S. Rudner, E. Berg, and E. Demler, Exploring topological phases with quantum walks, Phys. Rev. A **82**, 033429 (2010).

[20] J. Ambjørn, A. Görlich, J. Jurkiewicz, and R. Loll, Quantum gravity via causal dynamical triangulations, in *Springer Handbook of Spacetime* (Springer, New York, 2014), pp. 723–741.

[21] C. Rovelli and F. Vidotto, *Covariant Loop Quantum Gravity: An Elementary Introduction to Quantum Gravity and Spinfoam Theory* (Cambridge University Press, Cambridge, 2015).

[22] O. Duranthon and G. Di Molfetta, Coarse-grained quantum cellular automata, Phys. Rev. A **103**, 032224 (2021).

[23] Indeed, the full way to model the discrete curvature, including the singularities, is by considering the presence of dislocations, such as pentagonal and conical defects (e.g., 12 exactly for fullerenes) [28]. A systematic study of dislocations in the context of QWs has been extensively considered by one of the authors in an independent work.

[24] M. Manighalam and G. Di Molfetta, Continuous time limit of the DTQW in 2d+1 and plasticity, Quant. Info. Proc. **20**, 76 (2021).

[25] A. Sinha and R. Roychoudhury, Dirac equation in (1+1)-dimensional curved space-time, Int. J. Theor. Phys. **33**, 1511 (1994).

[26] H. Beiranvand and E. Rokrok, General relativity search algorithm: a global optimization approach, Int. J. Comput. Intell. Appl. **14**, 1550017 (2015).

[27] F. F. Moghaddam, R. F. Moghaddam, and M. Cheriet, Curved space optimization: A random search based on general relativity theory, arXiv:1208.2214.

[28] P. Schwerdtfeger, L. Wirz, and J. Avery, The topology of fullerenes, WIREs Comput. Mol. Sci. **5**, 96 (2015).

[29] https://github.com/vdng9338/qw_simul